Insect Biochemistry and Molecular Biology 106 (2019) 39–46

Contents lists available at ScienceDirect

Insect Biochemistry and Molecular Biology

journal homepage: www.elsevier.com/locate/ibmb

Clustered miR-2, miR-13a, miR-13b and miR-71 coordinately target *Notch* gene to regulate oogenesis of the migratory locust *Locusta migratoria*

Jiasheng Song, Wanwan Li, Haihong Zhao, Shutang Zhou*

Key Laboratory of Plant Stress Biology, State Key Laboratory of Cotton Biology, School of Life Sciences, Henan University, Kaifeng, 475004, China

ARTICLE INFO

Keywords:
miRNA cluster
Notch
Juvenile hormone
Female reproduction
Locust

ABSTRACT

MicroRNAs (miRNAs), ~22-nt small noncoding RNAs with a crucial role in various biological processes of organisms, are usually clustered in the genome. However, little is known about the miRNA clusters involved in insect reproduction. By small RNA sequencing and quantification followed by qRT-PCR, we found that the expression of invertebrate-specific miR-2/13/71 cluster including miR-2, miR-13a, miR-13b and miR-71 significantly decreased after adult ecdysis of the migratory locust, *Locusta migratoria*. Luciferase reporter assay and RNA immunoprecipitation demonstrated that miR-2/13/71 bound to the protein coding sequence of *Notch* and downregulated its expression. Injection of miR-2/13/71 agomiRs led to significant decrease of *Notch* expression as well as markedly reduced levels of *Vitellogenin* mRNA, suppressed oocyte maturation and impaired ovarian growth. Moreover, the expression of miR-2/13/71 was repressed by juvenile hormone (JH). Our results thus point to a previously unidentified mechanism by which JH-repressed miR-2/13/71 coordinately downregulates *Notch* to modulate insect reproduction. The increase of JH and decrease of miR-2/13/71 expression in both previtellogenic and vitellogenic stages of adult females ensure a high level of *Notch* expression, critically contributing to JH-dependent vitellogenesis and oogenesis.

1. Introduction

MicroRNAs (miRNAs) bind to the 3'-untranslated region (3'UTR) or the protein coding sequence (CDS) of their target mRNAs to regulate gene expression at the post-transcriptional level (Forman et al., 2008; Ghildiyal and Zamore, 2009; Rigoutsos, 2009). A typical feature of miRNA is that several miRNAs are often clustered in discrete genomic regions and polycistronically transcribed. miRNAs in the same cluster tend to regulate functionally related genes or genes in a signaling pathway (Hausser and Zavolan, 2014; Ventura et al., 2008; Wang et al., 2011, 2016). While extensive studies have been conducted on singly transcribed miRNAs, the regulatory role of clustered miRNAs in insect development, metamorphosis and reproductions is less understood (Belles, 2017; Belles et al., 2012; Lucas and Raikhel, 2013; Roy et al., 2018). The evolutionarily conserved let-7 cluster including let-7, miR-100 and miR-125 are transcriptionally activated by 20-hydroxyecdysone (20E) and its receptor EcR in *Drosophila melanogaster* (Chawla and Sokol, 2012; Hertel et al., 2012). During adult morphogenesis of *D. melanogaster*, let-7 and miR-125 target *abrupt* gene to regulate wing development (Caygill and Johnston, 2008). In the cockroach *Blattella germanica*, let-7 and miR-100 but not miR-125 modulate wing formation during nymphal-adult transition (Rubio and Belles, 2013). In the silkworm *Bombyx mori*, let-7 targets 20E-response genes *FTZ-F1* and *E74* for larval-pupal transition (Ling et al., 2014). The invertebrate-specific miR-2 cluster is comprised of miR-2 family members (miR-2, miR-13a and miR-13b) and miR-71 in many insect species (Campo-Paysaa et al., 2011; Wheeler et al., 2009). In *B. mori*, miR-2, miR-13a and miR-13b modulate wing morphogenesis via targeting *Abnormal wing disc* (*Awd*) and *Fringe* (*Fng*) genes (Ling et al., 2015). In *B. germanica*, miR-2 miRNAs scavenge *Krüppel-homolog 1* (*Kr-h1*) transcripts at the final nymphal instar, crucially contributing to the onset of metamorphosis (Lozano et al., 2015). Despite the reports on let-7 and miR-2 clusters that are involved in insect metamorphosis, how miRNA clusters function in insect reproduction remains an enigma.

Insect vitellogenesis and oogenesis are stimulated by juvenile hormone (JH) in a variety of insects. In dipteran insects like *D. melanogaster* and the mosquito *Aedes aegypti*, though 20E is the principle hormone governing Vitellogenin (Vg) synthesis, JH controls fat body competence for Vg synthesis in the mosquito (Raikhel et al., 2005; Roy et al., 2018) and Vg uptake by oocytes in *D. melanogaster* (Belles, 2005; Raikhel et al., 2005). In the red flour beetle *Tribolium castaneum*, JH regulates Vg synthesis in the fat body while 20E regulates ovarian growth and oocyte maturation (Parthasarathy et al., 2010; Sheng et al., 2011). In the primitive insects like *B. germanica* and the migratory locust *Locusta*

* Corresponding author.
E-mail address: szhou@henu.edu.cn (S. Zhou).

https://doi.org/10.1016/j.ibmb.2018.11.004
Received 10 September 2018; Received in revised form 15 November 2018; Accepted 15 November 2018
Available online 16 November 2018
0965-1748/

migratoria, JH appears to act independently of 20E to promote vitellogenesis and oocyte maturation (Raikhel et al., 2005; Song et al., 2014; Wang et al., 2017; Wyatt and Davey, 1996). Recent studies have demonstrated that miR-275, miR-1174, miR-1890, miR-277 and miR-8 play a pivotal role in 20E-dependent blood intake, blood digestion, lipid metabolism and Vg secretion in vitellogenic adult females of *Ae. aegypti*, and dysfunction of these miRNAs results in defective egg production (Bryant et al., 2010; Ling et al., 2017; Liu et al., 2014; Lucas et al., 2015a, 2015b). RNAi-mediated knockdown of *Dicer 1* and *Argonaute 1* (*Ago1*), the key regulators of miRNA biogenesis and function, causes severe defects in the oocyte maturation of *B. germanica* and *L. migratoria* (Song et al., 2013; Tanaka and Piulachs, 2012), indicating a crucial role of miRNAs in JH-dependent female reproduction. However, little has been done to explore the mechanisms of miRNA regulation in JH-dependent vitellogenesis and oogenesis.

The migratory locust is a favorite model for studying the underlying mechanisms of JH-dependent female reproduction, as JH controls locust Vg synthesis in the fat body, secretion into the hemolymph and uptake by the maturing oocytes (Guo et al., 2014; Luo et al., 2017; Wu et al., 2016; Wyatt and Davey, 1996). To identify miRNAs involved in locust vitellogenesis and oogenesis, we performed small RNA sequencing and quantification using fat bodies from adult female locusts on the day of eclosion as well as those in both previtellogenic and vitellogenic stages. We found that the expression levels of miR-2/13/71 cluster significantly reduced after adult emergence. JH downregulated miR-2/13/71 expression. Luciferase assays and RNA immunoprecipitation revealed that miR-2/13/71 bound the CDS of *Notch*. Notch plays a crucial role in insect oogenesis (Assa-Kunik et al., 2007; Baumer et al., 2012; Irles et al., 2016; Xu and Gridley, 2012; Xu et al., 1992), but its regulation by miRNAs in insects has not been determined. We demonstrated that miR-2/13/71 agomiR treatment resulted in significantly decreased levels of *Notch* expression, accompanied by reduced *Vg* transcripts, arrested oocyte maturation and blocked ovarian growth. Our study provides new insights into miRNA regulation in JH-dependent oogenesis and egg production.

2. Material and methods

2.1. Insects

The gregarious phase of migratory locust was reared under a 14L:10D photoperiod and at 30 ± 2 °C as previously described (Wang et al., 2017). The diet included a continuous supply of dry wheat bran with fresh wheat seedlings provided twice per day. JH-deprived adult female locusts were obtained by topical application of 500 μg (100 μg/μl dissolved in acetone) ethoxyprecocene (Sigma-Aldrich) per locust to inactivate corpora allata within 12 h after adult emergence (Dhadialla et al., 1987; Zhou et al., 2002). To restore JH activity, s-(+)-methoprene (Santa Cruz Biotech) was topically applied at 150 μg (30 μg/μl dissolved in acetone) per locust 10 d post ethoxyprecocene treatment (Dhadialla et al., 1987; Zhou et al., 2002).

2.2. Small RNA sequencing and miRNA cluster identification

Small RNA sequencing and quantification were performed with small RNA libraries derived from the fat body of adult females at 0, 2, 4 and 6 days post adult emergence, using the Illumina HiSeq 2500 platform. The clean reads were obtained by eliminating the low-quality reads, empty adapters, reads shorter than 18 nt, and reads with Poly(A) tail. Sequences of tRNA, rRNA, snRNA, snoRNA and piRNA were removed by similarity search using the Rfam12.1 and piRNABank database. miRNAs were identified by blasting the rest sequences with miRBase (V21.0) and referring to the locust genome (Wang et al., 2014). Clustered miRNAs were identified according to their genome positions. miRanda (V3.3a) (Enright et al., 2003), PITA (V6) and MicroTar (V0.9.6) (Thadani and Tammi, 2006) were employed for prediction of miRNA binding sites. The predicted target genes were then annotated and enriched in KEGG database in KOBAS 2.0 (Xie et al., 2011).

2.3. RNA extraction and qRT-PCR

Total RNA was isolated using TRIzol reagent (Thermo Fisher). For RNA or pri-miRNA quantification, cDNA was reverse transcribed with the FastQuant RT Kit (Tiangen). qRT-PCR was performed using a LightCycler 96 System and the SuperReal PreMix Plus kit (Tiangen), initiated at 95 °C for 2 min, followed by 40 cycles of 95 °C for 20 s, 58 °C for 20 s, and 68 °C for 20 s. For miRNA quantification, cDNA was synthesized from total RNA using miRNA first strand cDNA synthesis kit (Tiangen). qRT-PCR for miRNA was conducted using LightCycler system (Roche) and miRcute miRNA qPCR kit (Tiangen) at 94 °C for 2 min plus 40 cycles of 94 °C for 20 s and 60 °C for 34 s. The relative expression levels were calculated using the $2^{-\Delta\Delta Ct}$ method with β-actin and U6 as the internal controls of RNA and miRNA, respectively. Primers used for qRT-PCR were listed in Table S1.

2.4. Luciferase reporter assay

cDNA fragments with miRNA binding sties were cloned into pmirGLO vector (Promega) and confirmed by sequencing. For site mutation, the miRNA seed regions were mutated to their complementary sequences using Site-directed and Ligase-Independent Mutagenesis (Chiu et al., 2004). The mimic of *Caenorhabditis elegans* miRNA (sense: 5′-UUC UCC GAA CGU GUC ACG UTT-3′; antisense: 5′-ACG UGA CAC GUU CGG AGA ATT-3′) was used as the negative control (Sun et al., 2013; Wu et al., 2018). The recombinant vectors, miRNA mimics or the negative control (GenePharma) were then transfected into HEK293T cells using lipofectamine 3000 (Thermo Fisher). After 36 h, the luciferase activity was measured using the Dual-Glo Luciferase Assay System (Promega) and analyzed with GloMax 96 Microplate Luminometer (Promega). Primers used for site mutation were included in Table S1.

2.5. RNA immunoprecipitation (RIP)

RIP experiments were performed using Magna RIP Kit (Millipore) according to the manufacture's instruction. Briefly, freshly dissected fat bodies from adult females injected with miR-2/13/71 agomiRs or the agomiR of negative control were homogenized in ice-cold RIP lysis buffer, centrifuged for 15 min at 14,000 × *g*, and stored at −80 °C overnight. After further centrifugation for 15 min at 14,000 × *g*, the supernatant was incubated at 4 °C for 4 h with magnetic beads pre-incubated with a monoclonal antibody against locust Ago1 (Yang et al., 2014) or normal mouse IgG. The precipitated RNA was eluted and reverse transcribed to cDNA using Superscript IV reverse transcriptase and random hexamers (Thermo Fisher), followed by quantification using qRT-PCR. The agomiR of *C. elegans* miRNA (described in Section 2.4) was used as the negative control. The enrichment of *Notch* mRNAs by miR-2/13/71 agomiR treatment was calculated by normalizing with the IgG blank control and comparing with the negative control.

2.6. RNA interference (RNAi) and agomiR treatment

cDNA templates were amplified by PCR, cloned into pGM-T easy vector (Tiangen) and confirmed by sequencing. For RNAi experiments, dsRNA of Notch and green fluorescent protein (GFP) were synthesized using T7 RiboMAX Express RNAi system (Promega). Adult female locusts within 12 h after eclosion were intra-abdominally injected with 10 μg dsRNA and boosted on day 5. For agomiR treatment, adult females within 12 h after eclosion were intra-abdominally injected with 1 nmol agomiR (GenePharma) along with *in vivo* RNA Transfection Reagent (Engreen), and boosted twice on day 3 and day 6. The agomiR

of *C. elegans* miRNA described above was used as the negative control. Primers for dsRNA synthesis were included in Table S1.

2.7. Data analysis

Statistical analyses were performed by Student's *t*-test or One-way ANOVA with LSD (Least Significant Difference) post hoc test using the SPSS 21.0 software. Values were shown as Mean ± SEM and significant difference was considered at $P < 0.05$.

3. Results

3.1. Identification of miRNA clusters involved in locust vitellogenesis and oogenesis

The first gonadotrophic cycle of adult female locusts used in this study was approximately 9–10 days, and vitellogenesis started from approximately 5 days post adult eclosion (PAE). In search for miRNA clusters involved in locust vitellogenesis and oogenesis, we performed a comparative analysis of differential miRNA expression profiling with small RNA libraries derived from the fat body of adult female locusts within 12 h post adult eclosion (0 PAE) as well as those at 2, 4, 6 days PAE. In a total, 77 miRNAs in 28 clusters were identified, of which 4 clusters were comprised of evolutionary conserved miRNAs (Table S2; Fig. 1A). In this study, we chose to focus on the conserved miRNA clusters because of their crucial roles in insect development and reproduction as well as their conservation across insect orders. As shown in the right panel of Fig. 1A, compared to that on the day of adult eclosion, the expression of miR-3477/12 cluster significantly decreased at 2 days PAE, slightly elevated at 4 days PAE and dropped again at 6 days PAE. Interestingly, the expression levels of miR-2/13/71 cluster were significantly lower at 4–6 days PAE in comparison with that on day 0 (Fig. 1A). In contrast, the expression levels of miR-9/306 cluster were significantly higher at 4–6 days PAE compared to that on day 0 (Fig. 1A). With respect to miR-750/1175 cluster, their expression levels had no significant change from 0 to 6 days PAE (Fig. 1A).

Knowing that miR-2/13/71 expressed at significantly lower levels on day 4–6 relative to day 0 as shown by small RNA sequencing and quantification, we next performed qRT-PCR to further reveal the expression profiles of miR-2/13/71 using total RNAs isolated from the fat body of adult females during 0–8 days PAE. Compared to that on day 0, the expression levels of miR-2, miR-13a, miR-13b and miR-71 significantly decreased by 41.2–49.1%, 44.8–46.8%, 42.1–47.8% and 42.8–51.9%, respectively at 2–8 days PAE (Fig. 1B). However, no significant difference was seen among 2–8 days PAE (Fig. 1B). We also measured the temporal pattern of the primary transcripts of miR-2/13/71 cluster (pri-miRNA). Similar to mature miRNAs, the transcript levels of miR-2/13/71 pri-miRNA declined by 71.9–73.4% at 2–8 days PAE compared to that on day 0 (Fig. 1C). As locust hemolymph JH titers increase significantly during the previtellogenic stage and reach the peak in the vitellogenic phase (Guo et al., 2018), we further evaluated the responsiveness of miR-2/13/71 to JH using the 10-days-old adult females, ethoxyprecocene-treated adult females for 10 d and those further treated with methoprene for 6–48 h. When endogenous JH was deprived by ethoxyprecocene treatment, the expression levels of miR-13a and miR-71 significantly increased by 1.4- and 1.6-fold, respectively (Fig. 2A). With respect to miR-2 and miR-13b, their expression showed a tendency of increase in JH-deprived fat bodies compared to those at 10 days PAE (Fig. 2A) Further application of methoprene on JH-deprived adult females resulted in 33.5–39.6%, 24.7–30.5%, 31.9–35.8% and 20.6–24.7% decrease of miR-2, miR-13a, miR-13b and miR-71 expression levels, respectively at 24–48 h (Fig. 2B–E). Surprisingly, chemical allatectomy by ethoxyprecocene treatment failed to cause significant increase of miR-2 and miR-13b expression (Fig. 2A), whereas methoprene treatment led to significant decline of miR-2 and miR-13b expression (Fig. 2B and D). The data suggest that some miRNAs might differentially respond to the deprive of endogenous JH and the application of exogenous JH analogue. Similarly, while ethoxyprecocene treatment did not cause significant increase of miR-2/13/71 pri-miRNA transcripts (Fig. 2F), additional application of

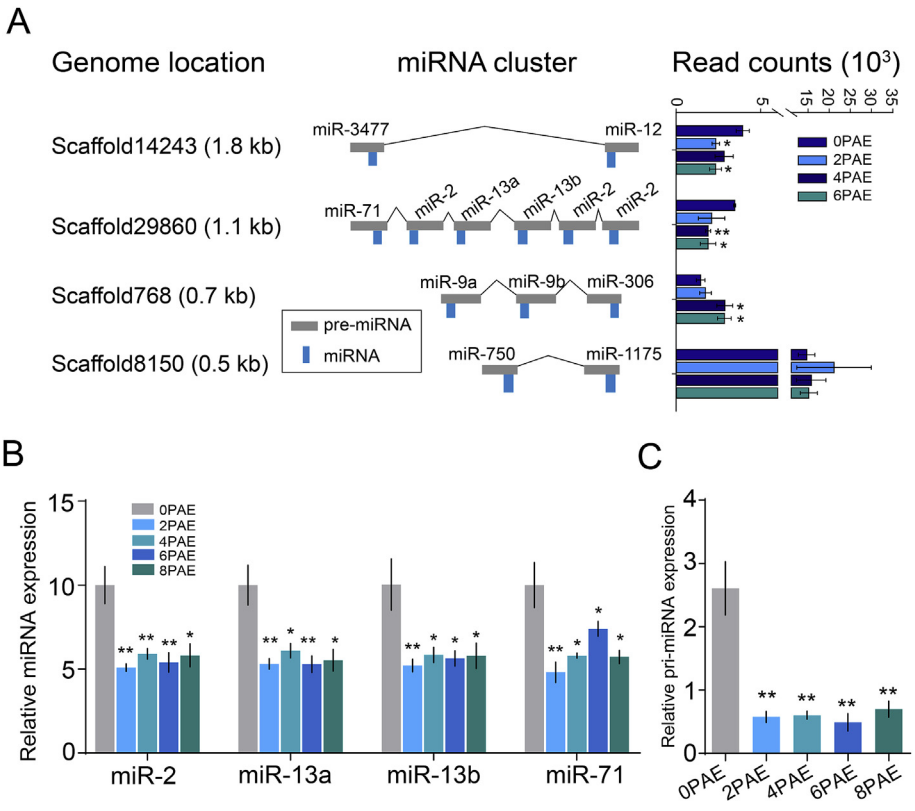

Fig. 1. Evolutionarily conserved miRNA clusters in vitellogenic adult females of *L. migratoria*. (A) The genome organization of 4 conserved miRNA clusters identified from small RNA sequencing and quantification. Left panel, the genome location and length of miRNA clusters. Middle panel, genome organization of miRNAs in the clusters. Gray rectangles indicate the precursor of miRNAs, and blue rectangles represent the mature miRNA. Right panel, the expression profiles of 4 conserved miRNA clusters in small RNA sequencing and quantification from the fat body of adult female locusts within 12 h post adult eclosion (0PAE) as well as those at 2, 4 and 6 days PAE. *, $P < 0.05$ and **, $P < 0.01$ compared to 0PAE. n = 3. (B, C) Temporal expression patterns of miR-2, miR-13a, miR-13b and miR-71 (B) as well as the pri-miRNA of miR-2/13/71 (C) in the fat body of adult females during the first gonadotrophic cycle. *, $P < 0.05$ and **, $P < 0.01$ compared to 0 PAE. n = 8. (For interpretation of the references to colour in this figure legend, the reader is referred to the Web version of this article.)

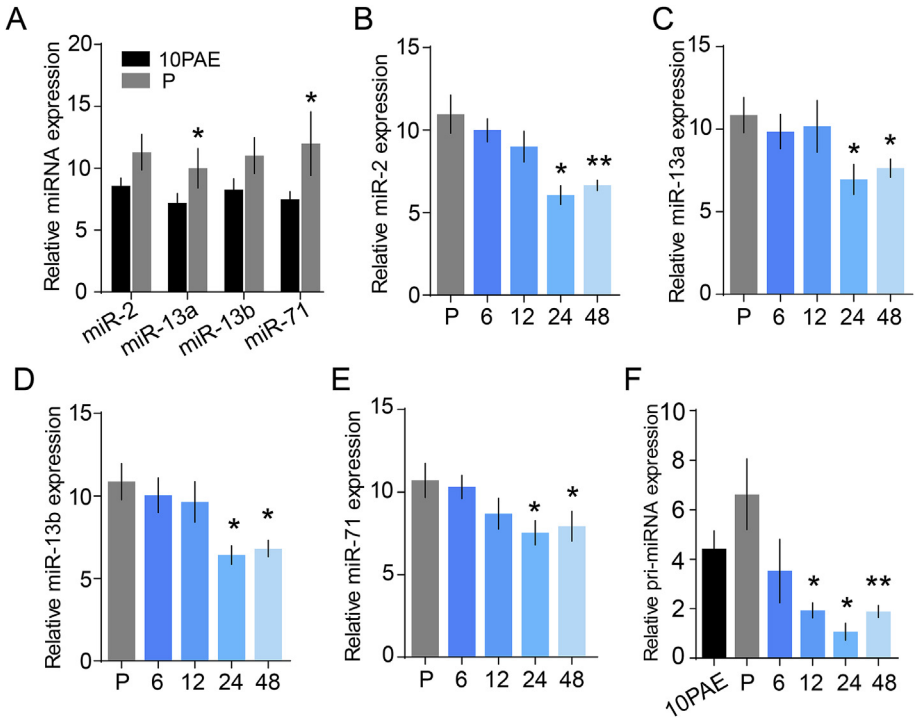

Fig. 2. Responseness of miR-2/13/71 expression to JH. (A) The relative expression levels of miR-2, miR-13a, miR-13b and miR-71 in the fat body of 10-days-old adult females (10PAE) and those treated with ethoxyprecocene for 10 days (P). *, $P < 0.05$ compared to 10PAE. n = 8. (B–E) The relative expression levels of miR-2 (B), miR-13a (C), miR-13b (D) and miR-71 (E) in the fat body of adult females treated with ethoxyprecocene for 10 days (P) and those further treated with methoprene for 6–48 h. *, $P < 0.05$ and **, $P < 0.01$ compared to the ethoxyprecocene treatment (P). n = 8. (F) The relative expression levels of miR-2/13/71 pri-miRNA in the fat body of 10-days-old adult females (10PAE), those treated with ethoxyprecocene for 10 days (P) and those further treated with methoprene for 6–48 h. *, $P < 0.05$ and **, $P < 0.01$ compared to the ethoxyprecocene treatment (P). n = 5.

methoprene resulted in 71.2–83.3% decrease of miR-2/13/71 pri-miRNA transcripts at 12–48 h (Fig. 2F). Collectively, these results suggest that miR-2/13/71 cluster transcribed in response to JH treatment. The decreased expression of miR-2/13/71 in the previtellogenic and vitellogenic stages suggests that the absence of miR-2/13/71 cluster is required for JH-dependent locust vitellogenesis and egg production.

3.2. miR-2/13/71 targets Notch during locust vitellogenesis and oogenesis

To decipher the underlying mechanisms of miR-2/13/71 regulation in locust vitellogenesis and oogenesis, we employed the algorithms of miRanda, PITA and MicroTar together with a locust transcriptome (Guo et al., 2014) to predict the potential target genes. Three members of miR-2/13/71, miR-2, miR-13a and miR-13b, belong to the miR-2 family (Marco et al., 2012), which have the same “seed” regions and high similarity of mature miRNA sequences (Fig. S1). As an initial step, miR-2 family was selected for target gene prediction. Among the predicted transcripts, 8 pathways were enriched by KEGG analyses, and Notch pathway was on the top (Fig. S2A). To further assess whether miR-2 family targets Notch pathway, we performed the binding site prediction using miRanda, PITA and MicroTar algorithms. As shown in Fig. S2B, *Notch*, *Fringe* (*Fng*), *Nicastrin* (*Ncstn*), *Anterior pharynx defective 1* (*Aph-1*), *Presenilin enhancer 2* (*Pen2*) and *Presenilin-2* (*Psen*) but not *Delta*, *Serrate* or *Tace* were predicted to be the target genes of miR-2, miR-13a and miR-13b. Next, we used miRanda, PITA and MicroTar to predict whether these genes are targets of miR-71, and found that miR-71 potentially binds to *Notch*, *Fng*, *Ncstn* and *Pen2* mRNAs.

To validate the binding of miR-2/13/71 to the predicted target genes in Notch pathway, we conducted dual-luciferase reporter assays by co-transfection of miRNA mimics and recombinant pmirGLO vector with ~500 bp cDNA fragments containing the predicted miRNA binding sites into HEK293T cells. When miR-2/13/71 mimics were transfected, the abundance of miR-2, miR-13a, miR-13b and miR-71 increased by 729-, 4349-, 4351- and 11,984-fold, respectively (Fig. 3A) compared to the control mimics (ck). After miR-2/13/71 mimics were co-transfected with the recombinant vector containing their binding sites of *Notch* (GenBank: MG213851), the reporter activities significantly reduced to 54.4% of the control levels (Fig. 3B). However, co-transfection of miR-2/13/71 mimics with the recombinant vectors containing their predicted binding sites of *Pen2* (GenBank: MG213852), *Psen* (GenBank: MH708142), *Aph-1* (GenBank: MH708138), *Ncstn* (GenBank: MH708141) or *Fng* (MG213853) had no significant effect on the reporter activity (Fig. 3B). When miR-2, miR-13a, miR-13b and miR-71 mimics were individually transfected with the constructed vectors containing the binding sites of *Notch*, reporter activities significantly decreased by 26.3%, 35.9%, 46.4% and 44.6%, respectively compared to the mimic controls (Fig. 3C). Again, individual transfection of miR-2, miR-13a, miR-13b and miR-71 mimics with the constructed vectors containing the binding sites of *Pen2*, *Psen*, *Aph-1*, *Ncstn* or *Fng* had no significant effect on the reporter activity (Fig. S2C). To further document the binding of miR-2, miR-13a, miR-13b and miR-71 to *Notch* mRNA, we mutated their binding sites complementary to the “seed” sequences (Fig. S3) for dual luciferase assays. As shown in Fig. 3C, the capacity of miR-2, miR-13a, miR-13b and miR-71 to inhibit the Notch reporter activity was blocked. Collectively, these data suggest that miR-2/13/71 bind to the CDS of *Notch* mRNA to repress its expression.

miRNA-Ago1 complex is an essential component of RNA-induced silence complex (RISC) for post-transcriptional regulation of target genes. We therefore performed RNA immunoprecipitation in the fat body using a monoclonal antibody against locust Ago1 (Yang et al., 2014) to determine the *in vivo* interaction of miR-2/13/71 and *Notch* mRNA. After miR-2/13/71 agomiR treatment, the levels of *Notch* mRNA significantly increased by 24.8-fold in the Ago1-precipitated RNAs compared to the agomiR of negative control (Fig. 3D). When miR-2, miR-13a, miR-13b and miR-71 agomiRs were individually applied, the precipitated levels of *Notch* mRNA were elevated by 20.6-, 23.5-, 22.4- and 24.6-fold, respectively when compared to the agomiR of negative control (Fig. 3E). Collectively, the above observations provide a clear indication that miR-2/13/71 bind to *Notch* mRNA.

3.3. miR-2/13/71 agomiR treatment suppresses locust vitellogenesis and oogenesis

To explore the role of miR-2/13/71 in locust vitellogenesis and oogenesis, agomiR was applied on adult females on day 0 (within 12 h

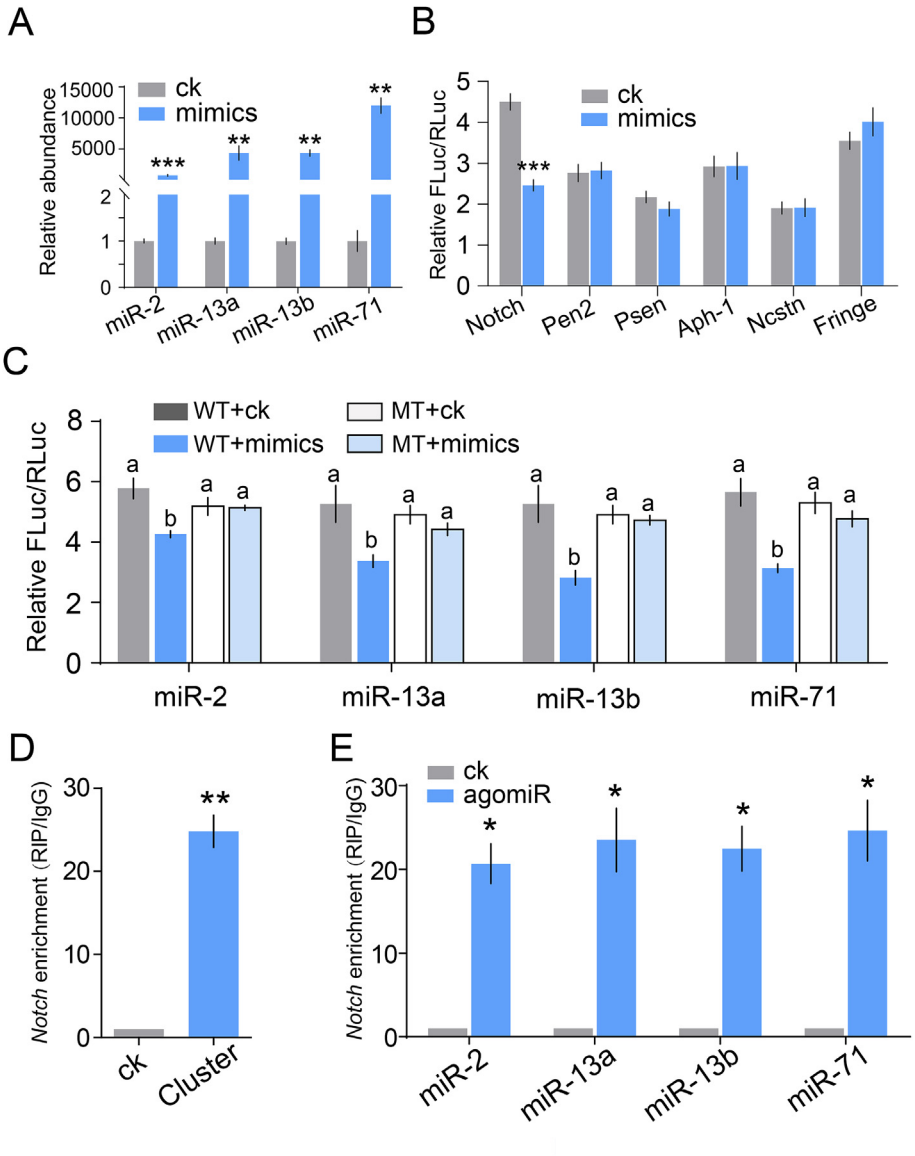

Fig. 3. *In vivo* binding and downregulation of *Notch* by miR-2/13/71. (A) Relative abundance of miR-2, miR-13a, miR-13b and miR-71 in HEK293 cells transfected with the respective miRNA mimics vs. the mimic of negative control (ck). **, $P < 0.01$ and ***, $P < 0.001$. n = 6. (B) Dual luciferase assays using HEK293T cells co-transfected with miR-2/13/71 mimics and recombinant pmirGLO vectors containing the predicted binding sites of *Notch*, *Pen2*, *Psen*, *Aph1*, *Ncstn* and *Fng*. ***, $P < 0.001$ compared to the negative control (ck). n = 6. (C) Dual luciferase reporter assays using HEK293T cells transfected with the respective mimics of miR-2, miR-13a, miR-13b, miR-71 and negative control (ck) plus recombinant pmirGLO vectors containing the predicted binding sites (WT) and mutated binding sites (MT) of *Notch*. Means labeled with different letters indicate the significant difference at $P < 0.05$. n = 6. (D) RNA immunoprecipitation showing the enrichment of *Notch* mRNA in the fat body of adult females injected with miR-2/13/71 agomiRs. **, $P < 0.01$ compared to the agomiR of negative control (ck). n = 3. (E) RNA immunoprecipitation showing the enrichment of *Notch* mRNA in the fat body of adult females injected individually with miR-2, miR-13a, miR-13b and miR-71 agomiRs. *, $P < 0.05$ compared to the agomiR of negative control (ck). n = 3.

post adult eclosion) and boosted twice on days 3 and 6. Phenotypes were examined at 8 days PAE, when Vg expression reached a peak and the primary oocytes were nearly matured. After miR-2/13/71 agomiR treatment, the levels of miR-2, miR-13a, miR-13b and miR-71 were increased by 63.5-, 74.2-, 71.2- and 65.6-fold, respectively in the fat body (Fig. 4A), leading to an average of 56.4% reduction of *Notch* transcripts (Fig. 4B). As a result, the mRNA levels of *VgA* (GenBank: KF171066) and *VgB* (GenBank: KX709496) significantly decreased by 83.7% and 62.1%, respectively in the fat body of agomiR-treated adult females compared to the agomiR of negative control (Fig. 4C). As shown in Fig. 4D, miR-2/13/71 agomiR treatment resulted in suppressed oocyte maturation and ovarian growth. Statistically, the average length × width index of primary oocytes significantly decreased by 52% after miR-2/13/71 agomiR treatment (Fig. 4E).

As mentioned above, miR-2, miR-13a and miR-13b belong to the miR-2 family (Marco et al., 2012). We next examined the effects of miR-2 and miR-71 on locust vitellogenesis and oogenesis by individual injection of miR-2 agomiR and miR-71 agomiR. Treatment of miR-2 agomiR gave rise to 79.8-fold increase of miR-2 abundance, while application of miR-71 agomiR caused 125.8-fold elevation of miR-71 levels in the fat body (Fig. 5A). As shown in Fig. 5B, *Notch* transcripts reduced by 77.9% and 59.1% in miR-2 agomiR- and miR-71 agomiR-treated fat bodies, respectively. Consequently, *VgA* and *VgB* expression levels decreased by 79.5% and 71.4%, respectively in the fat body treated with miR-2 agomiR, while miR-71 agomiR treatment led to 77.3% and 59.2% reduction of *VgA* and *VgB* transcripts, respectively (Fig. 5C and D). Injection of either miR-2 agomiR or miR-71 agomiR resulted in suppressed oocyte maturation and inhibited ovarian growth (Fig. 5E), underscored by significantly lower length × width index of primary oocytes in miR-2 agomiR- or miR-71 agomiR-treated adult females compared to the agomiR of negative control (Fig. 5F). Interestingly, the phenotypes caused by miR-71 agomiR treatment (Fig. 5E and F) appeared to be less severe than those resulted from simultaneous application of miR-2, miR-13a, miR-13b and miR-71 agomiRs (Fig. 4D and E). No significant difference was observed between miR-2 agomiR and miR-71 agomiR treatment (Fig. 5E and F). Taken together, these observations indicate that miR-2/13/71 cluster play a crucial role in JH-stimulated vitellogenesis and oocyte maturation in locusts.

Since the function of Notch in locust vitellogenesis and oogenesis was not previously explored, we performed *Notch* RNAi in parallel. In *Notch*-depleted fat bodies, *Notch* mRNA levels dropped to 3.3% of the dsGFP controls (Fig. 6A). Consequently, the mRNA level of *VgA* and *VgB* significantly reduced by 37.9% and 46.3%, respectively in the fat body (Fig. 6B). Compared to the dsGFP controls, *Notch*-depleted adult

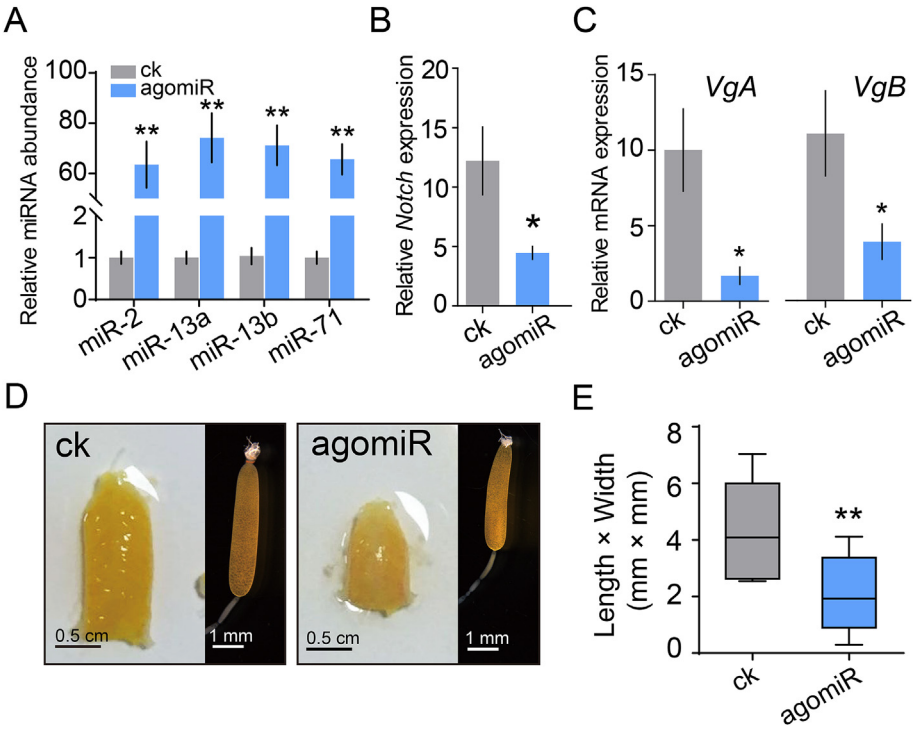

Fig. 4. Effect of miR-2/13/71 agomiR treatment on locust vitellogenesis and oogenesis. (A) Relative abundance of miR-2, miR-13a, miR-13b and miR-71 in the fat body of adult females injected with miR-2/13/71 agomiRs vs. the agomiR of negative control (ck). **, $P < 0.01$. n = 10. (B) Relative levels of *Notch* expression in the fat body of adult females treated with miR-2/13/71 agomiRs. *, $P < 0.05$ compared to ck. n = 10. (C) Relative levels of *VgA* and *VgB* expression in the fat body after miR-2/13/71 agomiR treatment. *, $P < 0.05$ compared to ck. n = 10. (D) Representative phenotypes of ovaries and primary oocytes after miR-2/13/71 agomiR treatment. ck, the agomiR of negative control. Scale bars: ovary, 0.5 cm; primary oocyte, 1 mm. (E) Statistical analysis for length × width index of primary oocytes. **, $P < 0.01$ compared to ck. n = 10.

females had blocked oocyte maturation and arrested ovarian growth (Fig. 6C). The average length × width index of primary oocytes was significantly decreased by 86% after *Notch* knockdown (Fig. 6D).

4. Discussion

4.1. The role of miR-2/13/71 in JH-dependent vitellogenesis and oogenesis

Previously, the function of miR-2/13/71 cluster in insects has been reported in three literature. In holometabolous *B. mori*, miR-2, miR-13a and miR-13b regulate *Awd* and *Fng* for wing morphogenesis during metamorphic pupal-adult transition (Ling et al., 2015). In hemimetabolous *B. germanica*, miR-2 family eliminates *Kr-h1* transcripts at the final nymphal instar, crucially contributing to the nymphal-adult metamorphosis (Lozano et al., 2015). In addition, miR-2, miR-13a and miR-13b act on two cytochrome P450 genes, *CYP9J35* and CYP325BG3 to regulate deltamethrin resistance in the mosquito *Culex pipiens pallens* (Guo et al., 2017). In the present study, dual luciferase assays using miR-2/13/71 mimics together with the wild-type and mutated binding sites of *Notch* showed that miR-2/13/71 inhibited the *Notch* reporter activity. RNA immunoprecipitation and subsequent qRT-PCR further documented the *in vivo* binding of miR-2/13/71 to *Notch* mRNA. Moreover, miR-2/13/71 agomiR treatment led to significantly decreased levels of *Notch* expression. Taken together, our study discovered a previously unidentified mechanism by which miR-2/13/71 bound to *Notch* mRNA and repressed its expression.

While a single miRNA or miRNA cluster has multiple target genes, a gene can be targeted by multiple miRNAs (Bonci et al., 2008;

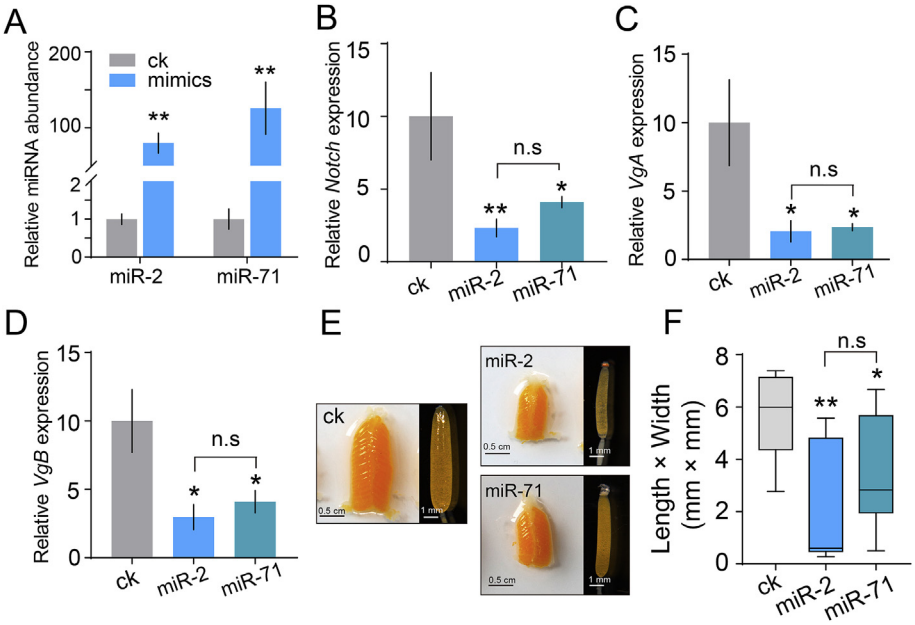

Fig. 5. Effect of miR-2 and miR-71 agomiR treatment on locust vitellogenesis and oogenesis. (A) Relative abundance of miR-2 and miR-71 in the fat body of adult females injected with miR-2 agomiR or miR-71 agomiR vs. the agomiR of negative control (ck). **, $P < 0.01$. n = 10. (B) Relative levels of *Notch* expression in the fat body of adult females injected with miR-2 agomiR or miR-71 agomiR. *, $P < 0.05$ and **, $P < 0.01$ compared to ck. n = 10. n.s, no significant difference. (C, D) Relative levels of *VgA* (C) and *VgB* (D) in the fat body of adult females injected with miR-2 agomiR or miR-71 agomiR. *, $P < 0.05$ compared to ck. n = 10. n.s, no significant difference. (E) Representative phenotypes of ovaries and primary oocytes after miR-2 agomiR or miR-71 agomiR treatment. ck, the agomiR of negative control. Scale bars: ovary, 0.5 cm; primary oocyte, 1 mm. (F) Statistical analysis for length × width index of primary oocytes. *, $P < 0.05$ and **, $P < 0.01$ compared to ck. n = 10.

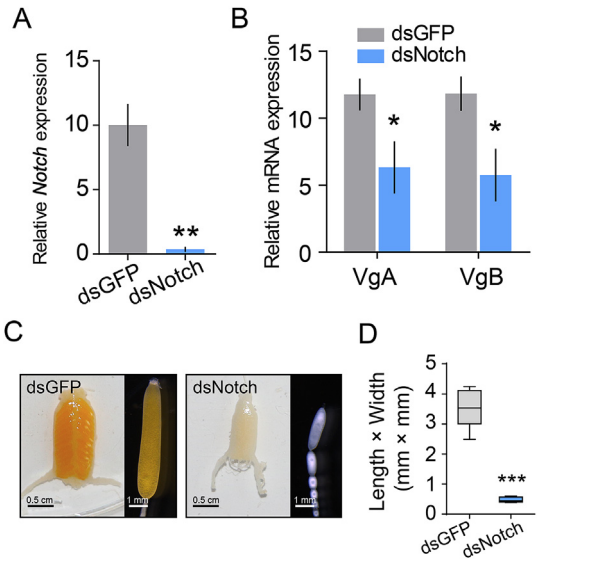

Fig. 6. Effect of *Notch* RNAi on locust vitellogenesis and oogenesis. (A) *Notch* knockdown efficiency in the fat body of adult females. dsNotch, *Notch* RNAi. **, $P < 0.01$ compared to the dsGFP control. n = 8. (B) Relative expression levels of *VgA* and *VgB* mRNA in the fat body of adult females after *Notch* RNAi. *, $P < 0.05$ compared to the dsGFP control. n = 8. (C) Representative phenotypes of ovaries and primary oocytes in *Notch*-depleted adult females vs. the dsGFP control. Scale bars: ovary, 0.5 cm; primary oocyte, 1 mm. (D) Statistical analysis for length × width index of primary oocyte. ***, $P < 0.001$ compared to the dsGFP control. n = 8.

Hashimoto et al., 2013). In human gastric cancer, miR-34 targets *Notch* to restrain tumorsphere formation and growth (Ji et al., 2008). *Notch* is also downregulated by the miR-200 family including miR-200a, miR-200b and miR-200c, consequently suppressing the TGF-β-mediated senescence, epithelial-to-mesenchymal transition and cancer stem cell functions (Ohashi et al., 2011). As well, miR-148a targets *Notch* to attenuate liver cancer via reducing tumor malignancy and liver fibrosis (Jung et al., 2016). In *D. melanogaster*, miR-1 modulates cardiac differentiation via targeting *Notch*, while miR-305 modifies homeostasis of intestinal stem cells through coordinating Notch and insulin signaling (Foronda et al., 2014; Kwon et al., 2005). Our present study therefore provides new insights into the downregulation of *Notch* by miR-2/13/71 in insects.

The expression of miR-2/13/71 significantly decreased in the fat body after adult eclosion, suggesting the requirement of miR-2/13/71 suppression in vitellogenic adult female locusts. Treatment of either miR-2 agomiR or miR-71 agomiR repressed locust vitellogenesis and oocyte maturation, but injection of miR-2/13/71 agomiRs resulted in severer defects in *Vg* expression, oocyte maturation and ovarian growth. These observations address the importance of miR-2/13/71 in locust vitellogenesis and oogenesis, which shed light on a new function of this miRNA cluster. Notably, the defective phenotypes of ovarian development and oocyte maturation caused by miR-2/13/71 agomiR treatment appeared to be less severe than that resulted from *Notch* RNAi, though miR-2/13/71 agomiR-treated adult females had relatively lower levels of *Vg* expression in the fat body than *Notch*-depleted groups. The results suggest that *Notch* RNAi might have more pronounced effect on ovaries, as Notch plays a pivotal role in ovarian development (Baumer et al., 2012; Irles et al., 2016; Xu and Gridley, 2012). It is also likely that application of miR-2/13/71 agomiRs might downregulate other genes controlling *Vg* expression in the fat body, consequently causing lower levels of *Vg* expression compared to *Notch* RNAi. It should be noted that the levels of *Notch* mRNA declined by 54% after miR-2/13/71 agomiR treatment, whereas *Notch* RNAi led to 97% reduction of *Notch* mRNA. The less defective phenotypes in the ovary of agomiR-treated adult females might be partially due to the relative higher levels of *Notch* transcripts.

4.2. Downregulation of miR-2/13/71 expression by JH

Intriguingly, the expression of miR-2/13/71 was repressed by JH. After adult ecdysis, the expression of miR-2/13/71 significantly declined, which opposites with the increased JH titer. The data indicate that the increased JH titer and declined abundance of miR-2/13/71 in both previtellogenic and vitellogenic stages ensure a high level of *Notch* expression, consequently contributing to JH-stimulated female reproduction. The suppressed expression of miRNAs by JH or 20E in insect metamorphosis and reproduction has been previously reported (Belles, 2017; Belles et al., 2012; Lucas and Raikhel, 2013; Roy et al., 2018). In *B. germanica*, JH-downregulated let-7 modulates wing formation during metamorphosis (Rubio and Belles, 2013; Rubio et al., 2012). In *D. melanogaster*, 20E inhibits miR-14 to elevate the levels of *EcR* expression and amplify 20E signaling (Varghese and Cohen, 2007). In *B. mori*, 20E represses the expression of miR-281 that targets *EcR-B* (Jiang et al., 2013). In vitellogenic adult females of *Ae. aegypti*, 20E-dependent expression of miR-275 and miR-1890 is required for blood digestion and ovarian development (Bryant et al., 2010; Lucas et al., 2015b). Thus, our results extend the view in hormonal regulation of miRNA during insect reproduction.

In summary, we demonstrated in this study that the evolutionarily conserved miR-2/13/71 cluster bound *Notch* mRNA and repressed its expression. Application of miR-2/13/71 agomiRs resulted in markedly reduced levels of *Vg* expression, accompanied by blocked oocyte maturation and impaired ovarian growth. The expression of miR-2/13/71 was repressed by JH and significantly reduced during previtellogenic development and vitellogenesis. The increase of JH and decline of miR-2/13/71 expression in vitellogenic adult females ensure a high level of *Notch* abundance, consequently contributing to successful egg production in locusts.

Acknowledgments

We thank Dr. Le Kang's lab for providing Ago1 antibody. This work was supported by the National Natural Science Foundation of China (NSFC) grants 31372258, 31702063 and 31630070).

Appendix A. Supplementary data

Supplementary data to this article can be found online at https://doi.org/10.1016/j.ibmb.2018.11.004.

References

Assa-Kunik, E., et al., 2007. *Drosophila* follicle cells are patterned by multiple levels of Notch signaling and antagonism between the Notch and JAK/STAT pathways. Development 134, 1161–1169.
Baumer, D., et al., 2012. Opposing effects of Notch-signaling in maintaining the proliferative state of follicle cells in the telotrophic ovary of the beetle *Tribolium*. Front. Zool. 9, 15.
Belles, X., 2005. Vitellogenesis directed by juvenile hormone. Reprod. Biol. Invertebr. 12 (Pt B 12), 157–197.
Belles, X., 2017. MicroRNAs and the evolution of insect metamorphosis. In: In: Berenbaum, M.R. (Ed.), Annual Review of Entomology, vol. 62. pp. 111–125.
Belles, X., et al., 2012. Insect MicroRNAs: from Molecular Mechanisms to Biological Roles. Elsevier Science B.V.
Bonci, D., et al., 2008. The miR-15a-miR-16-1 cluster controls prostate cancer by targeting multiple oncogenic activities. Nat. Med. 14, 1271–1277.
Bryant, B., et al., 2010. microRNA miR-275 is indispensable for blood digestion and egg development in the mosquito *Aedes aegypti*. Proc. Natl. Acad. Sci. U. S. A. 107, 22391–22398.
Campo-Paysaa, F., et al., 2011. microRNA complements in deuterostomes: origin and evolution of microRNAs. Evol. Dev. 13, 15–27.
Caygill, E.E., Johnston, L.A., 2008. Temporal regulation of metamorphic processes in *Drosophila* by the let-7 and miR-125 heterochronic microRNAs. Curr. Biol. 18, 943–950.
Chawla, G., Sokol, N.S., 2012. Hormonal activation of let-7-C microRNAs via EcR is required for adult Drosophila melanogaster morphology and function. Development

139, 1788–1797.
Chiu, J., et al., 2004. Site-directed, Ligase-Independent Mutagenesis (SLIM): a single-tube methodology approaching 100% efficiency in 4 h. Nucleic Acids Res. 32, e174.
Dhadialla, T.S., et al., 1987. Vitellogenin mRNA in locust fat body: coordinate induction of two genes by a juvenile hormone analog. Dev. Biol. 123, 108–114.
Enright, A.J., et al., 2003. MicroRNA targets in *Drosophila*. Genome Biol. 5, R1.
Forman, J.J., et al., 2008. A search for conserved sequences in coding regions reveals that the let-7 microRNA targets Dicer within its coding sequence. Proc. Natl. Acad. Sci. U. S. A. 105, 14879–14884.
Foronda, D., et al., 2014. Coordination of insulin and Notch pathway activities by microRNA miR-305 mediates adaptive homeostasis in the intestinal stem cells of the *Drosophila* gut. Genes Dev. 28, 2421–2431.
Ghildiyal, M., Zamore, P.D., 2009. Small silencing RNAs: an expanding universe. Nat. Rev. Genet. 10, 94–108.
Guo, Q., et al., 2017. The role of miR-2～13～71 cluster in resistance to deltamethrin in *Culex pipiens pallens*. Insect Biochem. Mol. Biol. 84, 15–22.
Guo, W., et al., 2018. Juvenile hormone-dependent Kazal-type serine protease inhibitor Greglin safeguards insect vitellogenesis and egg production. Faseb. J fj201801068R.
Guo, W., et al., 2014. Juvenile hormone-receptor complex acts on *Mcm4* and *Mcm7* to promote polyploidy and vitellogenesis in the migratory locust. PLoS Genet. 10.
Hashimoto, Y., et al., 2013. Multiple-to-multiple relationships between microRNAs and target genes in gastric cancer. PloS One 8, e62589.
Hausser, J., Zavolan, M., 2014. Identification and consequences of miRNA-target interactions–beyond repression of gene expression. Nat. Rev. Genet. 15, 599–612.
Hertel, J., et al., 2012. Evolution of the let-7 microRNA Family. RNA Biol. 9, 231–241.
Irles, P., et al., 2016. The Notch pathway regulates both the proliferation and differentiation of follicular cells in the panoistic ovary of *Blattella germanica*. Open Biol. 6, 150197.
Ji, Q., et al., 2008. Restoration of tumor suppressor miR-34 inhibits human p53-mutant gastric cancer tumorspheres. BMC Canc. 8, 266.
Jiang, J., et al., 2013. MicroRNA-281 regulates the expression of ecdysone receptor (EcR) isoform B in the silkworm, Bombyx mori. Insect Biochem. Mol. Biol. 43, 692–700.
Jung, K.H., et al., 2016. Differentiation therapy for hepatocellular carcinoma: multifaceted effects of miR-148a on tumor growth and phenotype and liver fibrosis. Hepatology 63, 864–879.
Kwon, C., et al., 2005. MicroRNA1 influences cardiac differentiation in *Drosophila* and regulates Notch signaling. Proc. Natl. Acad. Sci. U. S. A. 102, 18986–18991.
Ling, L., et al., 2014. MicroRNA Let-7 regulates molting and metamorphosis in the silkworm, *Bombyx mori*. Insect Biochem. Mol. Biol. 53, 13–21.
Ling, L., et al., 2015. MiR-2 family targets awd and fng to regulate wing morphogenesis in Bombyx mori. RNA Biol. 12, 742–748.
Ling, L., et al., 2017. MicroRNA-277 targets insulin-like peptides 7 and 8 to control lipid metabolism and reproduction in *Aedes aegypti* mosquitoes. Proc. Natl. Acad. Sci. U. S. A. 114 E8017-e8024.
Liu, S., et al., 2014. Mosquito-specific microRNA-1174 targets serine hydroxymethyltransferase to control key functions in the gut. Proc. Natl. Acad. Sci. U. S. A. 111, 14460–14465.
Lozano, J., et al., 2015. MiR-2 family regulates insect metamorphosis by controlling the juvenile hormone signaling pathway. Proc. Natl. Acad. Sci. U. S. A. 3740–3745 United States.
Lucas, K., Raikhel, A.S., 2013. Insect microRNAs: biogenesis, expression profiling and biological functions. Insect Biochem. Mol. Biol. 43, 24–38.
Lucas, K.J., et al., 2015a. MicroRNA-8 targets the Wingless signaling pathway in the female mosquito fat body to regulate reproductive processes. Proc. Natl. Acad. Sci. U. S. A. 112, 1440–1445.
Lucas, K.J., et al., 2015b. Mosquito-specific microRNA-1890 targets the juvenile hormone-regulated serine protease JHA15 in the female mosquito gut. RNA Biol. 12, 1383–1390.
Luo, M., et al., 2017. Juvenile hormone differentially regulates two Grp78 genes encoding protein chaperones required for insect fat body cell homeostasis and vitellogenesis. J. Biol. Chem. 292, 8823–8834.
Marco, A., et al., 2012. Evolution and function of the extended miR-2 microRNA family. RNA Biol. 9, 242–248.
Ohashi, S., et al., 2011. A NOTCH3-mediated squamous cell differentiation program limits expansion of EMT-competent cells that express the ZEB transcription factors. Cancer Res. 71, 6836–6847.
Parthasarathy, R., et al., 2010. Juvenile hormone regulation of vitellogenin synthesis in the red flour beetle, *Tribolium castaneum*. Insect Biochem. Mol. Biol. 40, 405–414.
Raikhel, A.S., et al., 2005. Hormonal control of reproductive processes. In: Gilbert, L.I. (Ed.), Comprehensive Molecular Insect Science. Elsevier, Amsterdam, pp. 433–491.
Rigoutsos, I., 2009. New tricks for animal microRNAS: targeting of amino acid coding regions at conserved and nonconserved sites. Cancer Res. 69, 3245–3248.
Roy, S., et al., 2018. Regulatory pathways controlling female insect reproduction. In: In: Berenbaum, M.R. (Ed.), Annual Review of Entomology, vol. 63. Annual Reviews, Palo Alto, pp. 489–511.
Rubio, M., Belles, X., 2013. Subtle roles of microRNAs let-7, miR-100 and miR-125 on wing morphogenesis in hemimetabolan metamorphosis. J. Insect Physiol. 59, 1089–1094.
Rubio, M., et al., 2012. MicroRNAs in metamorphic and non-metamorphic transitions in hemimetabolan insect metamorphosis. BMC Genomics 13.
Sheng, Z.T., et al., 2011. Juvenile hormone regulates vitellogenin gene expression through insulin-like peptide signaling pathway in the red flour beetle, *Tribolium castaneum*. J. Biol. Chem. 286, 41924–41936.
Song, J., et al., 2013. Argonaute 1 is indispensable for juvenile hormone mediated oogenesis in the migratory locust, *Locusta migratoria*. Insect Biochem. Mol. Biol. 43, 879–887.
Song, J., et al., 2014. Kruppel-homolog 1 mediates juvenile hormone action to promote vitellogenesis and oocyte maturation in the migratory locust. Insect Biochem. Mol. Biol. 52, 94–101.
Sun, Y., et al., 2013. MicroRNA-124 mediates the cholinergic anti-inflammatory action through inhibiting the production of pro-inflammatory cytokines. Cell Res. 23, 1270–1283.
Tanaka, E.D., Piulachs, M.D., 2012. Dicer-1 is a key enzyme in the regulation of oogenesis in panoistic ovaries. Biol. Cell. 104, 452–461.
Thadani, R., Tammi, M.T., 2006. MicroTar: predicting microRNA targets from RNA duplexes. BMC Bioinf. 7 (Suppl. 5), S20.
Varghese, J., Cohen, S.M., 2007. microRNA miR-14 acts to modulate a positive autoregulatory loop controlling steroid hormone signaling in *Drosophila*. Genes Dev. 21, 2277–2282.
Ventura, A., et al., 2008. Targeted deletion reveals essential and overlapping functions of the miR-17 through 92 family of miRNA clusters. Cell 132, 875–886.
Wang, J., et al., 2011. Regulatory coordination of clustered microRNAs based on microRNA-transcription factor regulatory network. BMC Syst. Biol. 5, 199.
Wang, X., et al., 2014. The locust genome provides insight into swarm formation and long-distance flight. Nat. Commun. 5, 2957.
Wang, Y., et al., 2016. microRNAs in the same clusters evolve to coordinately regulate functionally related genes. Mol. Biol. Evol. 33, 2232–2247.
Wang, Z., et al., 2017. An isoform of Taiman that contains a PRD-repeat motif is indispensable for transducing the vitellogenic juvenile hormone signal in *Locusta migratoria*. Insect Biochem. Mol. Biol. 82, 31–40.
Wheeler, B.M., et al., 2009. The deep evolution of metazoan microRNAs. Evol. Dev. 11, 50–68.
Wu, Y., et al., 2018. Transmembrane E3 ligase RNF183 mediates ER stress-induced apoptosis by degrading Bcl-xL. Proc. Natl. Acad. Sci. U. S. A. 115, E2762–e2771.
Wu, Z., et al., 2016. Juvenile hormone activates the transcription of cell-division-cycle 6 (Cdc6) for polyploidy-dependent insect vitellogenesis and oogenesis. J. Biol. Chem. 291, 5418–5427.
Wyatt, G.R., Davey, K.G., 1996. Cellular and molecular actions of juvenile hormone. II. Roles of juvenile hormone in adult insects. Adv. Insect Physiol. 26 26, 1–155.
Xie, C., et al., 2011. KOBAS 2.0: a web server for annotation and identification of enriched pathways and diseases. Nucleic Acids Res. 39, W316–W322.
Xu, J., Gridley, T., 2012. Notch signaling during oogenesis in *Drosophila melanogaster*. Genet. Res. Int. 2012, 648207.
Xu, T., et al., 1992. The involvement of the Notch locus in *Drosophila* oogenesis. Development 115, 913–922.
Yang, M., et al., 2014. MicroRNA-133 inhibits behavioral aggregation by controlling dopamine synthesis in locusts. PLoS Genet. 10, e1004206.
Zhou, S., et al., 2002. A locust DNA-binding protein involved in gene regulation by juvenile hormone. Mol. Cell. Endocrinol. 190, 177–185.